Macromolecules
ARTICLE

Macromolecules **2010**, *43*, 55–61 **55**
DOI: 10.1021/ma902095s

Novel Strategy To Design Magnetic, Molecular Imprinted Polymers with Well-Controlled Structure for the Application in Optical Sensors

Antonio L. Medina-Castillo,[†] Günter Mistlberger,*[,‡] Jorge F. Fernandez-Sanchez,*[,†] Antonio Segura-Carretero,[†] Ingo Klimant,[‡] and Alberto Fernandez-Gutierrez[†]

[†]*Department of Analytical Chemistry, Faculty of Sciences, University of Granada C/Fuentenueva, s/n 18071 Granada, Spain and* [‡]*Institute of Analytical Chemistry and Food Chemistry, Graz University of Technology, Stremayrgasse 16, 8010 Graz, Austria*

Received September 21, 2009; Revised Manuscript Received November 24, 2009

ABSTRACT: The incorporation of magnetic properties allows the in situ formation of sensor spots by magnetic separation and, consequently, optical readout from the outside. Several magnetic MIPs have been synthesized and characterized, highlighting that both the amount and distribution of magnetite are essential for producing a good material. This work also shows that well-organized structures must be obtained for designing magnetic MIP which can be used as optical sensors phases. Thus, in this work we propose a novel strategy to design well-organized, highly magnetic MIP particles to be used as optical sensing phases. The obtained magnetic MIP is the first one that has been used for optical sensing. It shows highly magnetic properties with high sensitivity (detection limit of 20 ng mL^{-1}), good imprinting effect (MIP/NIP ratio of 2.4), and high selectivity. This strategy may be further extended for implementing optical sensing phases in portable devices that can control a broad variety of analytes in different matrices (water, organic solvent, etc.) and may be used to improve sensitivity in other magnetic optical sensors.

Introduction

Molecular imprinting is a method of inducing molecular recognition properties in synthetic polymers in response to the presence of a template species during formation of the three-dimensional structure of a polymer.[1] The history of molecular imprinting is usually traced back to the experiments of Dickey in the 1940s and 1950s,[2,3] who was inspired to create affinity for dye molecules in silica gel by a theory of Linus Pauling as to how antibodies are formed.[4] Molecular imprinted polymers (MIPs) have been employed in a wide area.[5,6] Successful applications of MIPs were, e.g., in liquid chromatography, as material for solid-phase extraction, in membrane technology, for sensors, as artificial antibodies, in catalysis, in biotransformation processes, and as diagnostic tools for drug assays.[7] The main advantages over their natural competitors (i.e., antibodies) are their resistance to organic solvents and their stability over time, while maintaining the ability for molecular recognition. However, the application of MIPs for optical sensors was only successful in a few cases.[8−12] The three main reasons for this are (1) if the analyte is not fluorescent, it is challenging to find a good transducer, (2) the low sensitivity in many cases, and (3) the difficulty to implement the resulting MIPs in optical sensors.

While it is still difficult to find a transducer system for nonfluorescent analytes, the fixation of MIPs for luminescent analytes has been partly solved in the past with the following strategies. The first approach is based on the design of micro- or nanoparticles of MIPs and complex flow cells in which these particles are immobilized. This results in a sensor spot inside the cell which allows optical readout from the outside. However, sometimes fixing of the sensing material inside a cell can be cumbersome or even impossible. Alternatively, an additional polymer which works as a glue between MIP and fiber can be used, but it may change its optical and adsorption properties and thus its sensitivity and selectivity. All these problems can be minimized by the incorporation of magnetic properties into the sensing material. It allows the in situ formation of sensor spots by magnetic separation and, consequently, optical readout from the outside or an easy way to fix a MIP at the tip of an optical fiber.[13−15] Therefore, the incorporation of magnetic properties to MIPs by using paramagnetic magnetite (Fe_3O_4) nanobeads will simplify the readout of micro- or nanoparticles of MIPs with fiber-optic devices solving some of the previously mentioned drawbacks.

Several magnetic MIPs have been developed,[16,17] but none of them were proposed as optical sensor because, as we will demonstrate, the dark color of magnetite can cause severe problems in optical sensors. Magnetite is responsible for the filter effect and self-absorption of luminescence emission, decreasing the sensitivity or, in some cases, even annulling it.[13]

In this work, we evaluated three strategies for the preparation of magnetic MIPs (Mag-MIPs) for pyrene as model analyte. We show the relevance of the amount and the distribution of magnetite in MIPs for the performance of MIP-based optical sensors and propose a new strategy for designing highly magnetic, sensitive, and selective Mag-MIPs which can be used as magnetic optical sensors by measuring the intrinsic fluorescence of the target analyte; the analyte is selectively retained in the Mag-MIP and concentrated for readout by sensor spot formation.

Experimental Section

Reactives. Methyl methacrylate (MMA; 99%), divinylbenzene (DVB; 98%), ethylene glycol dimethacrylate (EDMA; 80% in meta/para isomers), 4-vinylpyridine (4-VP; 95%), 2,2′-azobis(isobutyronitrile) (AIBN), potassium persulfate (KPS), oleic acid (OA; 90%), sodium dodecyl sulfate (SDS; minimum 98.5% GC), and poly(vinyl alcohol) (PVA) were purchased

*Corresponding author: Ph +43 316 873 4324, Fax +43 316 873 4329, e-mail mistlberger@tugraz.at (G.M.); Ph +34 958243296, Fax +34 958249510, e-mail jffernan@ugr.es (J.F.F.-S.).

Published on Web 12/08/2009

from Sigma-Aldrich. Iron(II) chloride tetrahydrate ($FeCl_2 \cdot 4H_2O$) and iron(III) chloride hexahydrate ($FeCl_3 \cdot 6H_2O$) were obtained from Merck. Pyrene, acenaphthene (ACE), anthracene (ANT), fluorene (FLU), benzo[*a*]anthracene (BaA) and benzo[*a*]pyrene (BaP) were obtained from Fluka.

Magnetite coated with oleic acid: it was prepared according to the procedures described elsewhere.[14,18]

Chloroform Ferrofluid. It was prepared dispersing 2 g of magnetite coated with oleic acid in 40 mL of chloroform. This mixture was sonicated for 20 min, and then it was centrifuged at 6000 rpm for 15 min. The supernatant was further concentrated until the required concentration of magnetite was reached.

Mag-MIPs Prepared by Solution Polymerization (sMIP). A mixture containing 0.75 mL of a mixture of 83.5 mol % DVB, 16.5 mol % 4-VP, 26 mg of pyrene, 18 mg of AIBN, and 3 mL of chloroform ferrofluid with different weight of magnetite with respect to the weight of polymeric mixture (DVB and 4-VP) were placed in a glass vial. The mixtures were cooled with ice and purged with nitrogen for 3 min. The polymerization (65 °C, 24 h) resulted in a monolithic polymer which was ground in a ball mill, sieved through a 20 μm sieve, and washed several times with chloroform to extract the template.

Mag-MIPs Prepared by Emulsion Polymerization (eMIP). The discontinuous phase was based on a mixture of 0.75 mL of a mixture of 83.5 mol % DVB, 16.5 mol % 4-VP, 26 mg of pyrene, 18 mg of AIBN, and 3 mL of chloroform ferrofluid with different amounts of magnetite. The continuous phase was formed by 180 mg of PVA solved in 10 mL of Milli-Q water. The discontinuous phase was dispersed in a double-necked flask containing the continuous phase by vigorous mechanical stirring. It was purged with nitrogen, and the polymerization was carried out at 65 °C under a gentle stream of nitrogen for 24 h.

Magnetic Hybrid Nanoparticles Encapsulated by EDMA/MMA (EDMA/MMA-Fe_3O_4-OA). 2 g of lipophilic magnetic nanoparticles were dispersed in 5 mL of *n*-heptane and added to 400 mL of Milli-Q water containing 250 mg of SDS. The ice-cooled mixture was sonicated for 20 min in a high-energy sonifier (BRANSON, S-450D) at 70% amplitude for 20 min. The resulting miniemulsion was transferred slowly (under mechanical stirring) to a double-necked flask containing 1.5 mL of 40 wt % MMA and 60 wt % EDMA. The mixture was stirred for 2 h at room temperature. Then, 180 mg of KPS was added to start the polymerization, and the reaction system was heated to 65 °C under a gentle stream of nitrogen. After a polymerization time of 24 h the resulting product was washed 6 times with Milli-Q water, 5 times with acetone, and 5 times with chloroform in order to eliminate surfactant and unreacted compounds.

Magnetic Microparticle of MIP Containing EDMA/MMA-Fe_3O_4-OA Prepared by Precipitation Polymerization (pMIP). 0.75 mL of a mixture containing 83.5 mol % DVB, 16.5 mol % 4-VP 83, 26 mg of pyrene, and 18 mg of AIBN was mixed with 3 mL of a 6.5% (w/w polymer) methanolic dispersion of EDMA/MMA-Fe_3O_4-OA. The mixture was then placed in an ice-cooled glass vial and purged with nitrogen for 3 min. The polymerization was carried out at 65 °C for 24 h with continuous mechanical stirring.

Setup. The setup for the optical measurements consisted of a 1.5 mm diameter optical fiber probe (Varian Iberica, Spain) coupled with a special magnetic separator with an optimized geometry as described elsewhere.[15] Briefly, the separators consisted of four block magnets arranged like a star around the optical fiber with their like poles pointing against each other. The optical fiber probe was connected to the luminescence spectrometer (Varian Eclipse) by using a Varian fiber adapter. The Supporting Information shows a picture of the used setup (see Figure ESI-1).

Measuring Protocol. Samples were prepared by adding 0.7 mg of sensing material to a conventional quartz cuvette which contained 2 mL of the sample. The cuvette was shaken for 10 s prior to each measurement. The magnetic separator collected the Mag-MIPs at the tip of the optical fiber probe, and therefore, the luminescence intensity of the analyte bound to the Mag-MIPs was read out very efficiently (ESI shows an example for the data evaluation of the acquired measurements; see Figure ESI-2). As blank value (I_0) the same amount of particles was measured in 2 mL of solvent (water or acetonitrile/water mixture) without analyte. The analytical signal was obtained by subtracting I_0 from I_x.

To renew the sensing material, it was washed twice with 2 mL of acetone.

Results and Discussion

The incorporation of magnetic properties has been done by adding magnetite coated with oleic acid (Fe_3O_4-OA) which was prepared as described elsewhere.[14,18] 4-Vinylpyridine (4-VP) has been selected as functional monomer because it has a certain hydrophilic character and allows the dispersion of the material in water, and in addition, it favors the $\pi-\pi$ interactions during the formation of the prepolymerization complex with the template pyrene.[19] Divinylbenzene (DVB) has been used as cross-linker and chloroform as porogen and solvent.

In order to test how the amount and distribution of magnetite affects the optical recognition of pyrene, Mag-MIPs with different amounts of Fe_3O_4-OA (1, 2, and 5 wt %) were prepared by solution polymerization (sMIP) and emulsion polymerization (eMIP), and then they were evaluated. Nonimprinted polymers (NIP) were also prepared to distinguish between specific and unspecific interactions. The Fe_3O_4-OA distribution was studied by field-emission scanning electron microscopy with electron backscattering diffraction (FESEM-EBSD) in order to get a higher material contrast in the images (5 wt % Fe_3O_4-OA sMIP corresponds with Figure 1A and 5 wt % Fe_3O_4-OA eMIP with Figure 1B). The images elucidate an aggregation of the magnetite (white spots) in both cases. However, while in the sMIP the resulting magnetite clusters are evenly distributed in the particle, in the eMIP the clusters seem to be concentrated on the particles' surface. This morphology may be the result of a thermodynamic incompatibility between the employed polymeric phase and the magnetic ferrofluid. The low affinity between oleic acid coating of the magnetic nanoparticles (Fe_3O_4-OA) and the cross-linked polymer phase induces the phase separation between both.[20] Thus, the system organized itself to reach the most thermodynamically favored state corresponding to the minimum free energy for which the interfacial tensions between main phases were the lowest.[21,22]

While the sMIP particles show a homogeneous distribution along their entire surface, the distribution of the Fe_3O_4-OA aggregates in eMIP particles is more heterogeneous, obtaining some particles with a high and others with a low amount of magnetite. Moreover, the fraction of magnetite which is located close to the outer surface of the particles is even higher in eMIPs. Thus, the increased phase separation in eMIP compared to sMIP has an even more drastic effect on the optical sensitivity as we will show later. ESI shows the SEM pictures of 5 wt % Fe_3O_4-OA sMIP (Figure ESI-3) and 5 wt % Fe_3O_4-OA eMIP (Figure ESI-4).

There are three potential reasons for the increased phase separation between magnetite and polymer in eMIPs compared to sMIPs: (1) chloroform is a good dispersant for Fe_3O_4-OA nanoparticles, and the polymerization of sMIP was done in closed vials avoiding the chloroform evaporation while the eMIP polymerization was done under a gentle N_2 stream, making chloroform (the magnetite dispersant) evaporate faster; (2) the use of surfactant in the synthesis of the eMIP may increase the Fe_3O_4-OA diffusion to the contact surface with the aqueous medium, and therefore the separation of phases is more effective; and (3) the contact surface between the continuous phase

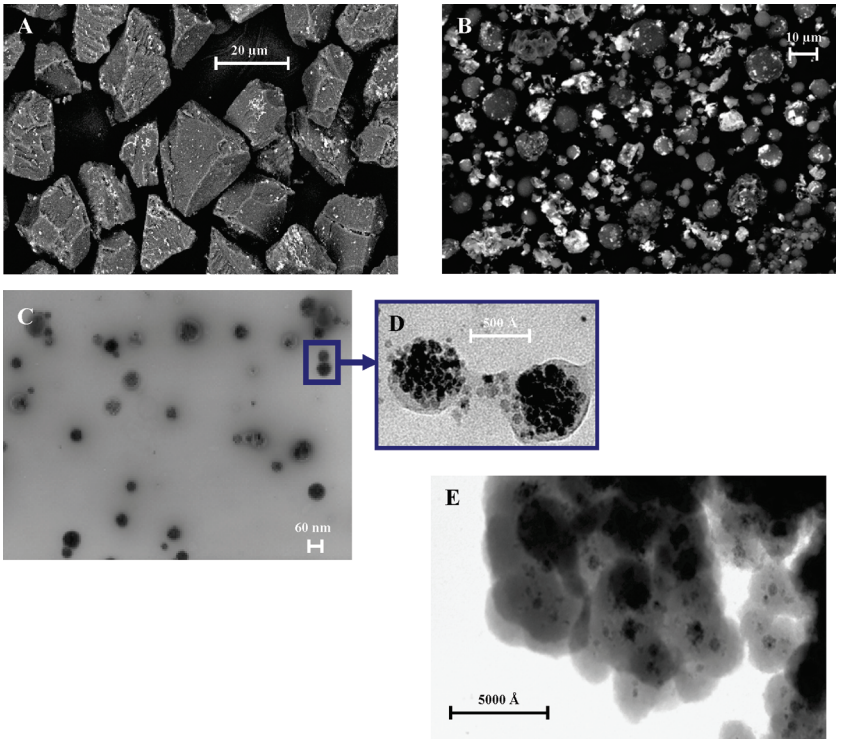

Figure 1. FESEM-EBDS pictures of (A) 5 wt % Fe_3O_4-OA sMIP and (B) 5 wt % Fe_3O_4-OA e-MIP. (C) TEM and (D) HREM pictures of EDMA/MMA-Fe_3O_4-OA nanoparticles. (E) HREM image of pMIP.

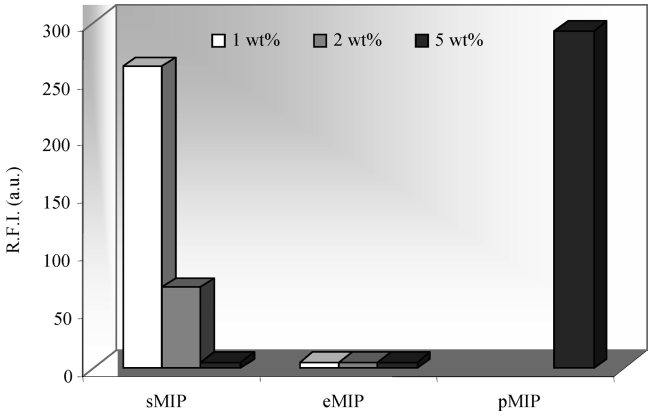

Figure 2. Effect of the Fe_3O_4-OA content on the optical sensitivity.

(containing water and surfactant) is very large in emulsion polymerizations. Therefore, the chances for magnetite to aggregate on the surface of the particles is higher, and once the magnetite found the thermodynamically more stable position at the surface, it will not drift back into the particle's interior.

All the Mag-MIPs containing 5 wt % Fe_3O_4-OA were highly magnetic and consequently collected very fast (within 2 min). Lower amounts of magnetite resulted in Mag-MIP which required more time for sensor spot formation. In addition, when the amount of magnetite is lower than 5 wt %, a lot of material is lost during the necessary washing steps.

In contrary, the absorption of the luminescence emission by the magnetite made the use of 5 wt % of Fe_3O_4-OA in pyrene sensitive Mag-MIPs impossible. 1 wt % Fe_3O_4-OA sMIP showed a response with pyrene which was not observed for higher percentages of magnetite, and in the case of eMIP, it was not possible to detect a response signal to pyrene at any percentage of (Fe_3O_4-OA) (see Figures 2 and 3b). As mentioned above, this was caused by the heterogeneous interparticle distribution of the

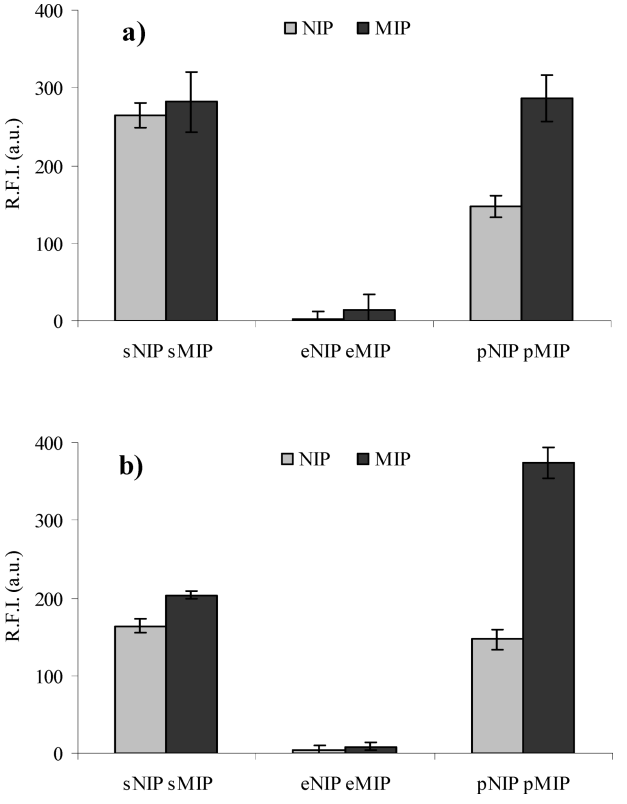

Figure 3. Relative fluorescence intensity (RFI) of pyrene immobilized in 1 wt % Fe_3O_4-OA s and e MIP and NIP and microparticles of pMIP and pNIP (5 wt % Fe_3O_4-OA) in (a) pure water, [pyrene] = 60 ng mL^{-1} and (b) 60% v/v acetonitrile/water mixture, [pyrene] = 1000 ng mL^{-1}.

magnetite and the high fraction of magnetite located at the outer surface of the particles (Figure 3b). Particles with a higher amount of Fe_3O_4-OA were collected faster in the field of view

of the optical fiber and created a highly absorbing layer which did not allow the coupling of luminescence light into the optical fiber.

In conclusion, for obtaining appropriate magnetic properties at least 5 wt % Fe_3O_4−OA were necessary. Magnetite had to be homogeneously distributed among the single particles, the phase separation had to be avoided, and the Fe_3O_4-OA had to be isolated from the MIP in order to avoid filter effects and self-absorption of luminescence emission.

Bearing in mind these conclusions, we propose the synthesis of new magnetic microparticles of MIPs in which the magnetite is located inside the particle, and the MIP is covering these magnetic cores. It allows the use of a higher amount of magnetite, and the isolation between magnetite and sensing material reduces the negative side effect of the magnetite on the sensitivity and selectivity of the MIP.

Figure 1E shows a HREM picture of this novel material (see Supporting Information, Figure ESI-5, which shows the size of the magnetic hybrid nanoparticles encapsulated by a cross-linked polymer into pMIP and also the SEM picture of pMIP). It was prepared in two steps. First, magnetic nanoparticles of Fe_3O_4-OA were encapsulated in a cross-linked polymer (EDMA/MMA) by a miniemulsion polymerization[23] (magnetic hybrid nanoparticles, see Figure 1C,D). Then, these magnetic particles were embedded into the structure of a MIP which was prepared by precipitation polymerization.[24] The resulting microparticles will be called pMIP (see Figure 1D). Nonimprinted polymer (pNIP) was prepared following the same protocol but in the absence of the template molecule pyrene.

The first step was the preparation of the magnetic hybrid nanoparticles encapsulated by a cross-linked polymer with specific features: small size (nanometer scale), high magnetite content[25−27] (between 80 and 90 wt %), and an appropriately cross-linked, polymeric matrix.

The cross-linked, polymeric matrix, which has to encapsulate the magnetic Fe_3O_4-OA nanoparticles, must be selected very carefully because interactions with the template, such as $\pi-\pi$ forces, must be avoided. A good choice of polymeric coating minimizes high background signals caused by irreversibly bound template molecules at the interface between the magnetic hybrid nanoparticles and the covering MIP.

In addition, these magnetic hybrid nanoparticles encapsulated by a cross-linked polymer must be dispersible in the medium in which the polymerization of the MIP will be carried out and have to have a high affinity to the MIP matrix in order to avoid the phase separation during the MIP formation in the second step.[28]

Methyl methacrylate (MMA) and ethylene glycol dimethacrylate (EDMA) were selected to encapsulate magnetic hybrid nanoparticles (40 wt % MMA−60 wt % EDMA) for the following reasons: they do not show $\pi-\pi$ interactions with pyrene, they provide a polymer which is dispersible in methanol, and the resulting cross-linked polymer has good affinity to the pMIP.

Parts C and D of Figure 1 show the TEM and HREM images of these magnetic hybrid nanoparticles encapsulated by EDMA/MMA (EDMA/MMA-Fe_3O_4-OA). They have a *z*-average of 63.7 nm with a polydispersity index (PDI) of 0.114 measured by dynamic light scattering. The estimated amount of iron oxide by electron microscopy in these nanoparticles is approximately between 75% and 90% (v/v) as can be seen in Figure 1C,D.

The second step was the preparation of MIP microparticles by precipitation polymerization in the presence of the EDMA/MMA-Fe_3O_4-OA nanoparticles prepared in the first step. MIP was prepared with 6.5 wt % of EDMA/MMA-Fe_3O_4-OA nanoparticles which corresponded approximately with a 5 wt % of Fe_3O_4-OA if an average Fe_3O_4-OA content of 80% is assumed in the EDMA/MMA-Fe_3O_4-OA nanoparticles. The yield in magnetic, molecular imprinted microparticles after several washes with chloroform in an ultrasonic bath was 92%.

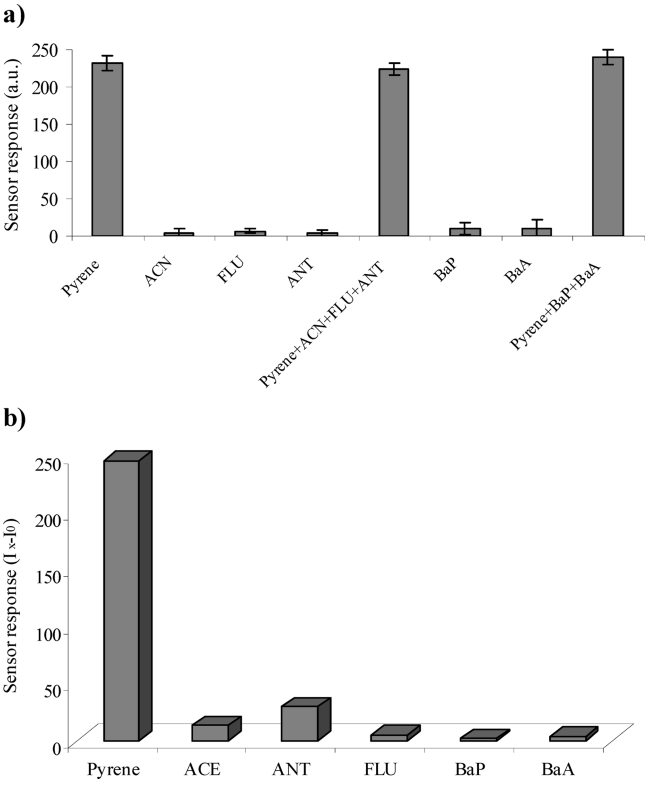

Figure 4. Optical interference study. (a) Study 1: sensing response ($I_x - I_0$) of pMIP in the presence of [pyrene] = [ACN] = [FLU] = [ANT] = 40 ng mL^{-1} and [BaA] = [BaP] = 1 ng mL^{-1} at the excitation and emission wavelengths of pyrene ($\lambda_{exc/em}$ = 340/396 nm). (b) Study 2: sensing response ($I_x - I_0$) of pMIP in the presence of [pyrene] = [ACN] = [FLU] = [ANT] = 40 ng mL^{-1} and [BaA] = [BaP] = 1 ng mL^{-1} at their respective excitation and emission wavelengths (see Table ESI-1 for the wavelengths).

Figure 1E shows the structure of the pMIP. The EDMA/MMA-Fe_3O_4-OA nanoparticles are homogeneously distributed in the pMIP. Thus, the surface of the resulting microparticles is free of magnetite. The phase separation is avoided by the adequate polarity of the EDMA/MMA-Fe_3O_4-OA nanoparticles which renders the free energy of the separation process along the polymerization process.

This new and well-organized material combines a high magnetite content (∼5 wt %) and adequate optical properties making it highly sensitive and selective. Figures 2, 3, and 4 show the analytical characteristics of pMIP. The time required for achieving a stable signal depends only on the speed of particle separation and, consequently, the magnetite content in the Mag-MIPs. The time required for analyte diffusion (response time) is much faster than the particle collection, and therefore its contribution to the overall equilibration time is negligible. This assumption is corroborated by the decreasing equilibration time from 1 wt % Fe_3O_4-OA sMIP to 5 wt % Fe_3O_4-OA pMIP (see Supporting Information, Figures ESI-6a and ESI-6c) and also by magnetization study at room temperature of pMIP and 1 wt % Fe_3O_4-OA sMIP (see Figure 5). It shows that the magnetic properties of pMIP are 3 times higher than of 1 wt % Fe_3O_4-OA sMIP.

Another big advantage of the novel pMIP is its higher sensitivity. Although pMIP contains 5 times more magnetite, the signal intensity of pMIP was higher than 1 wt % Fe_3O_4-OA sMIP at the same pyrene concentration. This was unexpected because the dark colored magnetite is absorbing light efficiently, and one would expect a decreasing intensity with an increasing magnetite concentration. The explanation is most probably a better optical isolation of the magnetite in pMIP from the

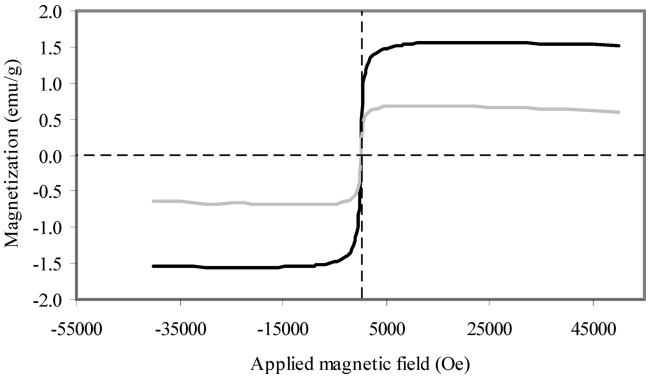

Figure 5. Magnetization curves at room temperature of pMIP (black line; S saturation magnetization is 1.52 emu g^{-1}) and 1 wt % Fe_3O_4-OA sMIP (gray line; saturation magnetization is 0.61 emu g^{-1}).

fluorescent analyte. pMIP showed a signal of 295 au for 65 ng mL^{-1} of pyrene in pure water while 1 wt % Fe_3O_4-OA sMIP provided only 262 units (see Figure 3a).

The new material also showed a good MIP/NIP ratio, i.e., the imprinting process was very effective: the MIP/NIP ratio in the determination of 1 mg L^{-1} pyrene solved in 60 wt % acetonitrile−water was 2.41 for pMIP compared to 1.30 for 1 wt % Fe_3O_4-OA sMIP (see Figure 3b) and 2.0 compared to 1.0 for 65 ng mL^{-1} pyrene in pure water (see Figure 3a). In the Supporting Information also the MIP/NIP ratio can be seen (Figure ESI-7). The increase of unspecific interactions in water was because water increases the unspecific hydrophobic interactions, mainly van der Waals forces, between pyrene and polymer. Thus, comparing MIP/NIP ratios of pMIP and sMIP, it is possible to suggest that phase separation and superficial distribution of Fe_3O_4-OA clusters during MIP formation might affect the imprinting phenomena in the MIP surface. This is more effective in a polymer with the surface free of Fe_3O_4-OA such as pMIP. The phase separation is a dynamic process which may adversely affect the adequate formation of molecular imprinting cavities during the polymerization: i.e., destroying the specific cavities and absorption of the template in the clusters of Fe_3O_4-OA.

To determine the sensitivity of pMIP to pyrene, a standard linear calibration graph was drawn according to recommended procedures (Figure ESI-8 shows the experimental results of the analytical calibration). The wide linear range, the small standard deviation, and the correlation coefficient close to unity indicate a good suitability of the obtained Mag-MIPs for analytical applications. The detection limit was determined using the IUPAC method (LOD = $3s_b/m$) where s_b is the standard deviation for 10 blank samples and m the slope of the calibration curve. The detection limit of 7 ng mL^{-1} shows the surprisingly high sensitivity of this magnetic optical sensor MIP.

In addition, the newly designed magnetic MIP microparticles were very selective to pyrene. Two different studies were developed. First, the signal of pyrene and the interference substances in pMIP were measured at the excitation and emission wavelengths which are optimal for pyrene. The plots in Figure 4a show that the optical signal of pyrene in pMIP was not affected by the presence of other luminescent PAHs such as acenaphthene (ACE), fluorene (FLU), anthracene (ANT), benzo[*a*]pyrene (BaP), and benzo[*a*]anthracene (BaA), and therefore it can be determined in the presence of these analytes (see also Supporting Information Figure ESI-9).

Second, the luminescent intensities of pyrene, ACE, FLU, ANT, BaP, and BaA were recorded at their respective excitation and emission wavelengths (see Table ESI-1). Figure 4b shows that the signals of the interferents (ACE, FLU, ANT, BaP, and BaP) were negligible, and therefore the selectivity of the sensing Mag-MIP was due to the imprinting phenomena and not caused by the spectroscopic characteristics of the analytes (see also Figure ESI-10). Thus, it is possible to conclude that the pMIP is highly selective to pyrene.

The affinity, capacity, and heterogeneity of pMIP have also been studied using the Freundlich isotherm-affinity distribution analysis. The aim of this study was double: on the one hand, to corroborate the high selectivity of pMIP by showing the affinity and capacity of pMIP to different PAHs; and on the other hand, to demonstrate the imprinting phenomena by analyzing the differences between pMIP and pNIP.

Because of the different hydrophobic character of PAHs (Supporting Information shows the solubility of the compounds under study, Table ESI-2), only three PAHs (FLU, ANT, and ACE) whose water solubility is higher than 50 ng mL^{-1} can be used to develop the cross-reactivity study because only they have the adequate solubility to be compared in the same range of affinities with pyrene (see Supporting Information for the linear ranges of these compounds in 60% v/v acetonitrile−water, Table ESI-3). The experimental binding data for this study were modeled with the Freundlich isotherm (FI) equation (see eq 1), which is a power function of concentration according to

$$B(C) = aC^m \tag{1}$$

where B and C are the concentrations of bound and free analyte, respectively, and a and m are fitting constants that have physical meaning.[29] The constant m is particularly interesting, as it is the heterogeneity index. Its value ranges from 0 to 1 and increases as heterogeneity decreases. The broad applicability of the FI to noncovalent MIPs has been demonstrated recently.[30]

Two additional binding parameters can be calculated:[31−35] the number of binding sites per gram of material ($N_{K_{min}-K_{max}}$; see eq 2) and the apparent average association constant ($\bar{K}_{K_{min}-K_{max}}$; see eq 3) where a and m are equivalent to Freundlich parameters:

$$N_{K_{min}-K_{max}} = a(1-m^2)(K_{min}^{-m} - K_{max}^{-m}) \tag{2}$$

$$\bar{K}_{K_{min}-K_{max}} = \left(\frac{m}{m-1}\right)\left(\frac{K_{min}^{1-m} - K_{max}^{1-m}}{K_{min}^{-m} - K_{max}^{-m}}\right) \tag{3}$$

The values for these parameters can be calculated for any range of binding affinities within the limits of the K_{min} and K_{max} being equal to the reciprocal corresponding concentrations $K_{min} = 1/C_{mim}$ and $K_{max} = 1/C_{max}$. Comparisons of $N_{K_{min}-K_{max}}$ and values are valid if the range of affinities considered in the calculation of these values are the same for all compared cases.[31,35]

All the isotherms were acquired in a 50% (v/v) mixture of acetonitrile and water, using 6 mg of polymer per 5 mL of solution of the target compound. The measurements were done after 1 h because the equilibrium was reached in 3 min due to the fast diffusion of the compounds into the pMIP (see Supporting Information Figure ESI-6c).

The Supporting Information shows all the experimental data of this study (see Figure ESI-11) which are summarized in Table 1.

Here, it can be seen that the value of pyrene adsorbed on pMIP particles is slightly higher than for the interferents, and consequently, the interaction pyrene−pMIP is the most effective one of the studied analytes. This means the prepared Mag-pMIP contains steric cavities with adequate geometry for pyrene. The small differences between the values of indicate a low binding energy of the prepolymerization complex due to the low energy forces (i.e., $\pi-\pi$ interactions) involved in the formation of the steric

Table 1. Freundlich Fitting Parameters, Weighted Average Affinity, and Number of Sites for Pyrene in pMIP and pNIP and ANT, FLU, and ACE in pMIP

	m	a [(μg g^{-1}) (L mg^{-1})^m]	r^2	$N_{K_{min}-K_{max}}{}^a$ (μmol g^{-1})] $\times 10^{-3}$	$K_{K_{min}-K_{max}}{}^a$ (L mol^{-1}) $\times 10^{-8}$
pyrene in pMIP	0.73 ± 0.02	331.82 ± 2.80	0.999	168.0 ± 1.0	12.0 ± 0.9
pyrene in pNIP	0.92 ± 0.04	214.31 ± 3.86	0.996	32.5 ± 0.6	11.0 ± 0.9
ANT in pMIP	0.95 ± 0.02	152.57 ± 3.29	0.999	14.4 ± 0.3	10.0 ± 0.9
FLU in pMIP	0.96 ± 0.01	162.19 ± 1.50	0.999	12.3 ± 0.1	9.0 ± 0.9
ACE in pMIP	0.99 ± 0.03	99.91 ± 1.90	0.998	1.9 ± 0.0	8.0 ± 0.8

[a] Calculated for a concentration range log $K = 1 - 0.53$ (mg L^{-1}).

binding cavities.[9] For this reason, pMIP can be cleaned very easily by only two washing steps with acetone.

The data also show that $N_{K_{min}-K_{max}}$ of pyrene in pMIP is 5 times higher than in pNIP. This means that the number of sites with adequate geometry and good accessibility to pyrene is higher in pMIP than in pNIP, demonstrating the imprinting phenomenon. In addition, $N_{K_{min}-K_{max}}$ of pyrene in pMIP was 89, 14, and 12 times higher than ACE, FLU, and ANT in pMIP, respectively. Therefore, pMIP particles were highly selective to pyrene and the steric cavities formed in pMIP had adequate geometry to pyrene, which was experimentally confirmed by optical interference measurements where none of the PAHs tested interfere with the selective determination of pyrene and none of them are observed at their maxima excitation and emission wavelengths (see Figure 4).

Conclusions

We have demonstrated a new synthetic route to a well-controlled magnetic imprinted material based on a two-step process: first, the incorporation of the magnetite into a matrix which does not negatively influence the molecular imprinting phenomenon and, second, the embedding of these magnetic nano precursors in the MIP structure which can be used for optical sensing. To the best of our knowledge, this is the first time that a magnetic MIP can be used as optical sensor.

The preparation of these microparticles is simple and provides a sensing material which is highly magnetic (content of 5 wt % Fe_3O_4-OA approximately) and sensitive (detection limit of 7 ng mL^{-1}). In addition, this material shows a very high affinity characteristic to pyrene which was the imprinted molecule (ratio MIP/NIP of 2.41, the highest and $N_{K_{min}-K_{max}}$ of pyrene in pMIP 5, 89, 14, and 12 times higher than pyrene in pNIP and ACE, FLU, and ANT in pMIP) and, therefore, very high selectivity. None of the tested luminescent PAHs (ACE, FLU, ANT, BaP, and BaA) interfered with the determination of pyrene.

Lastly, this novel strategy to design MIPs with well-controlled structure for the usage as optical sensors with adequate magnetic and optical properties may be further extended for implementing optical sensing phases in portable devices that can control a broad variety of analytes in different matrices (water, organic solvent, etc.) and may be used to improve sensitivity in other magnetic optical sensors.

Acknowledgment. The authors thank the Spanish Ministry of Education (FPU grant reference AP2006-01144 and Project CTQ2008-01394) and the Regional Government of Andalusia (Excellence projects P07-FQM-02738 and P07-FQM-02625) for their financial support.

Supporting Information Available: Additional SEM and HREM pictures; response of sMIP, eMIP, and pMIP to pyrene; calibration curve of pMIP with pyrene, MIP/NIP ratio; luminescenct characteristics of PAHs under study; optical interference studies; isotherm study: explanations of measuring protocol and setup.

This material is available free of charge via the Internet at http://pubs.acs.org.

References and Notes

(1) Sellergren, B. *Molecularly Imprinted Polymers, Man-Made Mimics of Antibodies and Their Applications in Analytical Chemistry, Techniques and Instrumentation in Analytical Chemistry*; Elsevier: Amsterdam, 2001.
(2) Dickey, F. H. The preparation of specific adsorbents. *Proc. Natl. Acad. Sci. U.S.A.* **1949**, *35* (5), 227–229.
(3) Dickey, F. H. Specific adsorption. *J. Phys. Chem.* **1955**, *59* (8), 695–707.
(4) Pauling, L. A theory of the structure and process of formation of antibodies. *J. Am. Chem. Soc.* **1940**, *62*, 2643–2657.
(5) Katz, A.; Davis, M. E. Molecular imprinting of bulk, microporous silica. *Nature* **2000**, *403* (6767), 286–289.
(6) Mayes, A. G.; Whitcombe, M. J. Synthetic strategies for the generation of molecularly imprinted organic polymers. *Adv. Drug Delivery Rev.* **2005**, *57* (12), 1742–1778.
(7) Masci, G.; Aulenta, F.; Crescenzi, V. Uniform-sized clenbuterol molecularly imprinted polymers prepared with methacrylic acid or acrylamide as an interacting monomer. *J. Appl. Polym. Sci.* **2002**, *83* (12), 2660–2668.
(8) Dickert, F. L.; Achatz, P.; Halikias, K. Double molecular imprinting - a new sensor concept for improving selectivity in the of polycyclic aromatic hydrocarbons (PAHs) in water. *Fresenius J. Anal. Chem.* **2001**, *371* (1), 11–15.
(9) Dickert, F. L.; Besenbock, H.; Tortschanoff, M. Molecular imprinting through van der Waals interactions: Fluorescence detection of PAHs in water. *Adv. Mater.* **1998**, *10* (2), 149–.
(10) Kirsch, N.; Hart, J. P.; Bird, D. J.; Luxton, R. W.; McCalley, D. V. Towards the development of molecularly imprinted polymer based screen-printed sensors for metabolites of PAHs. *Analyst* **2001**, *126* (11), 1936–1941.
(11) Sanchez-Barragan, I.; Costa-Fernandez, J. M.; Pereiro, R.; Sanz-Medel, A.; Salinas, A.; Segura, A.; Fernandez-Gutierrez, A.; Ballesteros, A.; Gonzalez, J. M. Molecularly imprinted polymers based on iodinated monomers for selective room-temperature phosphorescence optosensing of fluoranthene in water. *Anal. Chem.* **2005**, *77* (21), 7005–7011.
(12) Valero-Navarro, A.; Salinas-Castillo, A.; Fernandez-Sanchez, J. F.; Segura-Carretero, A.; Mallavia, R.; Fernandez-Gutierrez, A. The development of a MIP-optosensor for the detection of monoamine naphthalenes in drinking water. *Biosens. Bioelectron.* **2009**, *24* (7), 2305–2311.
(13) Chojnacki, P.; Mistlberger, G.; Klimant, I. Separable magnetic sensors for the optical determination of oxygen. *Angew. Chem., Int. Ed.* **2007**, *46* (46), 8850–8853.
(14) Mistlberger, G.; Borisov, S. M.; Klimant, I. Enhancing performance in optical sensing with magnetic nanoparticles. *Sens. Actuators, B* **2009**, *139* (1), 174–180.
(15) Mistlberger, G.; Chojnacki, P.; Klimant, I. Magnetic sensor particles: an optimized magnetic separator with an optical window. *J. Phys. D: Appl. Phys.* **2008**, *41*, 8.
(16) Wang, X. B.; Ding, X. B.; Zheng, Z. H.; Hu, X. H.; Cheng, X.; Peng, Y. X. Magnetic molecularly imprinted polymer particles synthesized by suspension polymerization in silicone oil. *Macromol. Rapid Commun.* **2006**, *27* (14), 1180–1184.
(17) Zhang, Y.; Liu, R.; Hu, Y.; Li, G. Microwave Heating in Preparation of Magnetic Molecularly Imprinted Polymer Beads for Trace Triazines Analysis in Complicated Samples. *Anal. Chem.* **2009**, *81* (3), 967–976.
(18) Zheng, W.; Gao, F.; Gu, H. Magnetic polymer nanospheres with high and uniform magnetite content. *J. Magn. Magn. Mater.* **2005**, *288*, 403–410.
(19) Baggiani, C.; Anfossi, L.; Baravalle, P.; Giovannoli, C.; Giraudi, G. Molecular recognition of polycyclic aromatic hydrocarbons by pyrene-imprinted microspheres. *Anal. Bioanal. Chem.* **2007**, *389* (2), 413–422.

(20) Montagne, F.; Mondain-Monval, O.; Pichot, C.; Elaissari, A. Highly magnetic latexes from submicrometer oil in water ferrofluid emulsions. *J. Polym. Sci., Part A: Polym. Chem.* **2006**, *44* (8), 2642–2656.
(21) Berg, J.; Sundberg, D.; Kronberg, B. *Polym. Mater. Sci. Eng.* **1986**, *54*, 367.
(22) Chen, Y. C.; Dimonie, V.; Elaasser, M. S. Interfacial phenomena controlling particle morphology of composite latexes. *J. Appl. Polym. Sci.* **1991**, *42* (4), 1049–1063.
(23) Gong, T.; Yang, D.; Hu, J. H.; Yang, W. L.; Wang, C. C.; Lu, J. Q. Preparation of monodispersed hybrid nanospheres with high magnetite content from uniform Fe_3O_4 clusters. *Colloids Surf., A* **2009**, *339* (1−3), 232–239.
(24) Odian, G. *Principles of Polymerization*, 4th ed.; Wiley-Interscience: Hoboken, NJ, 2004.
(25) Liu, X. Q.; Guan, Y. P.; Ma, Z. Y.; Liu, H. Z. Surface modification and characterization of magnetic polymer nanospheres prepared by miniemulsion polymerization. *Langmuir* **2004**, *20* (23), 10278–10282.
(26) Ugelstad, J.; Soderberg, L.; Berge, A.; Bergstrom, J. Monodisperse polymer particles - a step forward for chromatography. *Nature* **1983**, *303* (5912), 95–96.
(27) Xu, H.; Cui, L. L.; Tong, N. H.; Gu, H. C. Development of high magnetization Fe3O4/polystyrene/silica nanospheres via combined miniemulsion/emulsion polymerization. *J. Am. Chem. Soc.* **2006**, *128* (49), 15582–15583.
(28) Medina-Castillo, A.; Fernandez-Sanchez, J. F.; Segura Carretero, A.; Fernandez Gutierrez, A. A semi-empirical model to simplify the synthesis of homogeneous and transparent cross-linked polymers and their application in the preparation of optical sensing films. *Biosens. Bioelectron.* **2009**, *25*, 442−449.
(29) Jaroniec, M.; Madey, R. *Physical Adsorption on Heterogeneous Solids*; Elsevier: New York, 1988.
(30) Umpleby, R. J.; Baxter, S. C.; Bode, M.; Berch, J. K.; Shah, R. N.; Shimizu, K. D. Application of the Freundlich adsorption isotherm in the characterization of molecularly imprinted polymers. *Anal. Chim. Acta* **2001**, *435* (1), 35–42.
(31) Corton, E.; Garcia-Calzon, J. A.; Diaz-Garcia, M. E. Kinetics and binding properties of cloramphenicol imprinted polymers. *J. Non-Cryst. Solids* **2007**, *353* (8−10), 974–980.
(32) Garcia-Calzon, J. A.; Diaz-Garcia, M. E. Characterization of binding sites in molecularly imprinted polymers. *Sens. Actuators, B* **2007**, *123* (2), 1180–1194.
(33) Rampey, A. M.; Umpleby, R. J.; Rushton, G. T.; Iseman, J. C.; Shah, R. N.; Shimizu, K. D. Characterization of the Imprint Effect and the Influence of Imprinting Conditions on Affinity, Capacity, and Heterogeneity in Molecularly Imprinted Polymers Using the Freundlich Isotherm-Affinity Distribution Analysis. *Anal. Chem.* **2004**, *76* (4), 1123–1133.
(34) Sips, R. On the structure of a catalyst surface. 2. *J. Chem. Phys.* **1950**, *18* (8), 1024–1026.
(35) Spivak, D. A. Optimization, evaluation, and characterization of molecularly imprinted polymers. *Adv. Drug Delivery Rev.* **2005**, *57* (12), 1779–1794.